American Journal of Sciences and Engineering Research

E-ISSN -2348 – 703X, Volume 8, Issue 3, 2025

Epidemiology of Hepatitis D from 2018 to 2021 in the Iraq: using GIS Approach

Mohanad G. Murad

Basic science Department, College of Dentistry, University of Kufa, Al-Najaf, Iraq

---

Abstract: *The Department of Health and Life Statistics recently released the hepatitis D prevalence for each contiguous Iraqi province for a 4-year period, from 2018 to 2021. 4765.44 cases per 100,000 females and 5152.24 cases per 100,000 men were reported. From 2018 to 2021, county-based hepatitis D cases were subjected to a hotspot analysis utilizing Anselin Local Moran's I and Getis-Ord Gi* to find geographic clusters of those with greater rates for cases per 100,000. According to the results of Anselin Local Moran's I, three H-H clustering regions (hot spots) were observed for men in 2018/2019: Diyala and, Wasit, and Karbala (P=0.025) and Diyala, Babil, and Karbala (P=0.030). Fortunately none hot spot clustering area was found in 2021In 2018, the L-H outlier area (cold spot) was identified as Baghdad and Babil (P=0.006). In 2019, Baghdad was similarly the L-H outlier area (cold spot) (p=0.014). Baghdad and Karbala were the L-H outlier area (cold spot) for 2020 (p=0.034). The L-H outlier area (cold spot) determined in 2018 was Baghdad and Babil (p=0.005), while the three H-H clusters areas (hot spots) for females in 2018/2019 were Diyala, Wasit, and Karbala in Iraq (P=0.028) and Diyala, Babil, and Karbala (P=0.022). In 2019, Baghdad became likewise the L-H outlier area (cold spot) (p=0.006). The L-H outlier area (cold spot) for 2020–2021 was found in the Diyal and Karbala (p=0.040) and Karbala in Iraq (p=0.016). According to a Getis-Ord Gi* analysis, Basrah and Dhaqar were categorized as cold spot locations, which have a low rate of hepatitis D disease, while Diyala, Baghdad, Wasit, Babil, and Karbala were classified as hotspot areas, which had a high rates of hepatitis D disease.*

Key words: *Hepatitis D, GIS, Iraq, Getis-Ord Gi*, Anselin Local Moran's I.*

I. Introduction

Because it depends on HBV to exist, hepatitis type D (HDV) is regarded as a subviral satellite [1]. Over the last ten years, the number of Iraqi cases of hepatitis has grown. An increase of three times has been reported in HAV cases between 2009 and 2014. Iraq is thought of as having a low endemic rate for HBV and HCV when compared to its neighbors. The security situation and overcrowding of refugees and migrants in Iraq may be the cause of the rising prevalence of all kinds of hepatitis, as well as the lack of vaccine availability [2]. The virus poses a serious risk to the welfare of people since it can infect liver cells and proliferate indefinitely [3,4]. Weakness, anorexia, nausea, distension of the abdomen, and liver pain are among the disease's clinical signs. Spider nodes, laminitis, spleen swelling, chronic liver illness, and aberrant or prolonged liver function can potentially be signs of serious disease, which can be mild, moderate, or severe, based on how it presents clinically. In a stable external environment, HBV can persist for almost seven days and is extremely spreading, spreading from contact with blood and other body fluids [5]. To obtain an updated comprehension of the geographic distribution of hepatitis D in Iraq, this study made use of the Getis-Ord Gi* and Anselin Local Moran's I features of geographical Information Systems (GIS). For this study, information on Iraq's hepatitis D epidemic

 Received-12-05-2025, Accepted - 24-05-2025

rate was acquired from 2018 to 2021. geographical clustering study and an examination of the geographical distribution patterns of viral hepatitis D across several Iraqi provinces were conducted using Geographic Information Systems (GIS). This study advances our knowledge of the spatial epidemiologic features of hepatitis D and offers a solid scientific basis for creating specialized prevention and control measures.

II. Materials and Methods

The Central Bureau of Statistics provided us with population estimates, and the Department of Health and Life Statistics supplied us with the number of hepatitis D cases for each county in contiguous Iraq for the four-year period 2018–2021. The Najaf Urban Planning department's latitude and longitude measurements were used to specify each county's geographic center location (shapefile). We applied Anselin Local Moran's I and Getis-Ord Gi* to a hotspot analysis. Anselin Local Moran's I finds spatial clusters of features with different values, whereas Getis-Ord Gi* finds significant geographically cluster of high values (hotspots) with a low value (cold spots) [6].When examining geographical problems, it is customary to examine spatial patterns on a given collection of data utilizing a number of spatial statistical approaches [7]. In order to confirm the validity of the results, we utilized Getis-Ord Gi* and Anselin Local Moran's I to recognize hotspot barangays. ArcGIS 10.8 geographic information system software was used for both investigations, producing maps that showed Najaf city's a hotspot and cold spots using clustered and outlier analysis. This GIS application enables the execution of several strategies to identify the groupings present in the area under examination. The use of these methods has already been widely documented in the relevant literature since the 1980s, typically in studies that spend on finding local [14,15] and synthetic [8–13] indicators as well as in comparisons that take those geostatistical indications into account [14,15]. The applicable literature states that a number of specific methods would use the spatial autocorrelation calculation at a local level to reveal groupings. To examine the patterns of adaptations distribution of wealth, the hot spots analysis (based on Gi* de Getis-Ord) and clustering and outlier assessment (estimated on Anselin local Moran's I) have been employed. According to previous research, these geostatistical approaches are complimentary even if their views are essentially distinct [16,17]. Identifying clusters within a region is the aim of the hotspot study. These categories can indicate the highs and lows values of a specific variable, which correspond to hot and cold patches, respectively. The Mapping Clusters tool, which is part of ArcGIS's Geographic Statistics Tools suite, can be used to carry out the hot spot analysis (Getis-Ord Gi*), which is being done to identify those locations. This method is specified by a numerical equation [18] that follows:

$$G_i^* = \frac{\sum_{j=1}^{n} w_{i,j} w_j - \bar{X} \sum_{j=1}^{n} w_{i,j}}{s\sqrt{\frac{\left[n \sum_{j=1}^{n} w_{i,j}{}^2 - \left(\sum_{i,j}^{n} w_{i,j}\right)^2\right]}{n-1}}} \quad (1)$$

where x_j is the attribute value for feature j; $w_{i,j}$ is the spatial weight between feature i and j; n is equal to the total number of features and:

$$\bar{X} = \frac{\sum_{j=1}^{n} x_j}{n} S = \sqrt{\frac{\sum_{j=1}^{n} x_j^2}{n} - (\bar{X})^2}$$

In contrast, the cluster and outlier evaluation use the closeness criterion to find groups or aberrant data. Five different geographic class types are identified by this research. On the one hand, this approach finds locations with values that are either high or low in relation to their environment. Conversely, anomalous areas are identified by the study when a spot's value differs significantly from that of its neighbors, either much higher or lower. Additionally, there are instances in which no connections may be created. ArcGIS [19] uses the following mathematical approach for this analysis:

$$I_i = \frac{x_i - \bar{X}}{S_i^{\,2}} \sum_{j=1, j\neq i}^{n} w_{i,j}\left(x_j - \bar{X}\right) \ (2)$$

where x_i is an attribute for feature i, $\bar{X}$is the mean of the corresponding attribute, $x_{i,j}$is the spatial weight between feature $i\ and\ j$, and:

$$S_i^2 = \frac{\sum_{j=1, j\neq i}^{n}\left(x_j - \bar{X}\right)^2}{n-1}$$

With n equating to the total number of features.

III. Results and discussions

Table 1 displays Iraq's hepatitis D infection rates from 2018 to 2021. 4765.44 cases per 100,000 females and 5152.24 incidences per 100,000 men were reported. Male rates ranged from 0 to 321.69, while female rates ranged from 0 to 309.70. Fig. 1 displays the geographical diversity of Hepatitis D rates at the national level. The number of viral hepatitis D cases in Iraq increased by 7.53% over a 4-year period, from 1081.27 instances reported in 2018 to 1469.04 reported cases in 2021 for men. 71.56 instances each 100,000 people was the average incident rate. In contrast, there were 1059.91 reported cases of hepatitis D in 2018 and 25.77 reported cases in 2021 for females, indicating a 3.53% rise in cases during a 4-year period. 66.19 cases per 100,000 individuals was the average incidence rate. Northeast and southwest Iraq had the highest impact between 2018 and 2021. North and South Iraq had the lowest incidences. The hepatitis D geographic clustering map is shown in Figure 2. Throughout small regions, spatial autocorrelation has been investigated using the Moran index. Three H-H clustering regions (hot spots) were found for men in 2018/2019 (Fig. 2, left panel): Diyala, Wasit, and the city of Karbala (P=0.025) and Diyala, Babil, and Karbala (P=0.030). However, none hot spot clustering area was found in 2021. The L-H outlier location (cold spot) noticed in 2018 is Baghdad and Babil (P=0.006). In 2019, Baghdad was likewise the L-H outlier area (cold spot) (p=0.014). The L-H outlier area (cold spot) forecast 2020 identified between Karbala and Baghdad (p=0.034) (Table 2). Three H-H clustering regions (hot spots) were identified for females in 2018/2019 (Fig.2, right panel): Diyala, Wasit, and Karbala (P=0.028), Diyala, Babil, and Karbala (P=0.022), and Baghdad and Babil (p=0.005), which were identified as the L-H outlier area (cold spot) in 2018. In 2019, Baghdad was likewise the L-H outlier area (cold spot) (p=0.006). The L-H outlying area (cold spot) for 2020–2021 was found in the Diyal and Karbala had (p=0.040) as well as Karbala (p=0.016) (Table 2). According to the analysis, Basrah and Dhaqar were categorized as cold spot areas, which have a low disease incidence, whereas Diyala, Baghdad, Wasit, Babil, and Karbala were classified as hotspot areas, which have a high disease incidence. The results of the local hotspot analysis showed that there were in fact four cold hotspot areas for the regional autocorrelation of hepatitis D development nationwide. (Fig. 3, male left, female right panel, Table 3,4).

IV. Conclusions

Our spatial analysis's findings showed that hepatitis D prevalence was substantially concentrated across Iraq. The local Moran's equation I index showed low-incidence areas close to other high-incidence areas and high-incidence regions adjacent to other regions with a high incidence. The hotspot analysis found that the highest incidence rates were seen in Diyala, Baghdad, Wasit, Babil, and Karbala. the highest rate of inflation, which may be caused by local lifestyle and customs, economic expansion, health concerns, and personal opinions. To halt and control the spread of diseases including those caused by hepatitis D virus, the government must closely monitor and implement effective interventions, such as timely immunization and locally appropriate preventative measures.

Table 1. The Hepatitis D among Males and Females Rate/100,000 in the Iraq, 2018 to 2021.

		2018		2019		2020		2021			
FID	**Name**	**Male**	**Female**	**Male**	**Female**	**Male**	**Female**	**Male**	**Female**	**x/m**	**y/m**
0	Ninawa	6.24	12.12	31.04	32.41	34.93	24.51	74.25	19.60	272791.49	3989302.13
1	Dahuk	0.00	0.00	0.15	0.15	0.60	0.91	3.76	3.17	334379.27	4103395.39
2	Najaf	77.78	82.46	195.58	196.66	162.56	114.59	215.52	171.29	387011.64	3443996.29
3	Karbala	237.09	206.68	110.75	113.02	34.83	32.05	19.33	20.79	389130.23	3597406.85
4	Tam'mim	45.06	35.24	73.89	75.52	101.27	77.36	135.43	137.40	421468.60	3912621.45
5	Baghdad	57.63	51.99	59.24	60.87	48.20	56.98	45.56	47.51	442889.49	3682327.10
6	Muthanna	2.89	1.43	14.19	13.81	19.24	14.52	12.27	9.29	536921.59	3339553.17
7	Babil	22.88	22.60	155.66	156.89	120.74	91.18	167.80	121.70	463407.21	3598643.13
8	Diwaniyah	26.35	27.39	40.58	41.08	14.97	10.96	42.23	36.52	506051.66	3526126.49
9	Dha qar	72.73	56.77	37.52	37.35	13.71	20.73	26.31	33.33	627925.35	3453539.40
10	Basrah	16.60	17.23	5.27	5.25	2.13	1.82	9.14	7.20	730444.71	3364653.92
11	Salah ad din	63.36	61.84	234.94	239.44	166.02	141.82	244.73	213.77	373440.77	3824105.96
12	Anbar	0.00	0.00	61.45	64.69	106.30	101.68	146.44	135.61	183775.05	3653023.80
13	Arbil	0.00	0.00	0.00	0.00	0.00	0.00	0.83	0.53	428674.82	4022476.05
14	Diyala	110.15	148.89	241.75	246.54	115.10	139.51	191.09	173.54	509926.50	3757546.00
15	Sulaymaniyah	2.88	3.07	36.84	36.97	2.43	2.61	7.30	6.22	528343.85	3932819.32
16	Wasit	321.69	309.70	125.99	138.15	145.31	119.60	75.03	71.36	568831.86	3614655.33
17	Maysan	17.93	22.51	46.76	45.37	42.01	22.34	52.03	19.37	694529.24	3530861.37

Table2. Spatial Distribution of Clustering and Outlier Analysis for Males (2018-2021).

Clusters/ Outlier	Year's males	Approximate location	LMiZScore	LMiPValue	Observed /100,000
HH/LH	2018	Diyala, Wasit, and Karbala/Baghdad and Babil	1.934/-2.386	0.025/0.006	668/79
HH/LH	2019	Diyala, Babil, and Karbala/Baghdad	2.016/-2.560	0.030/0.014	506/59
LH	2020	Baghdad and Karbala	-1.898	0.034	82

Table3. Spatial Distribution of Clustering and Outlier Analysis for Females (2018-2021).

Clusters/ Outlier	Year's female	Approximate location	LMiZScore	LMiPValue	Observed /100,000
HH/LH	2018	Diyala, Wasit, and Karbala/Baghdad and Babil	1.918/-2.634	0.028/0.005	663/73
HH/LH	2019	Diyala, babil, and Karbala/Baghdad	2.006/-2.732	0.022/0.006	515/60
HH/LH	2020	Diyala and Baghdad/Karbala	1.932/-2.310	0.028/0.016	195/32

LH	2021	Diyal and Karbala	-2.138/ -1.867	0.022/ 0.040	6/20

Table4. Spatial Distribution of Hot spot and Cold spot Analysis for Males (2018-2021).

Clusters Analysis	**Year's Males**	**Approximate location**	**GiZScore**	**GiPValue**	**Observed /100,000**
Hot spot 99%	2018	Diyala, Baghdad, Wasit, Babil, and Karbala	2.319	0.024	747
Hot spot 95%	2019	Diyala, Baghdad, Babil, and Karbala	2.446	0.020	565
Hot spot 90%/ Cold spot 90%	2020	Diyala, Baghdad, and Karbala/ Basrah	1.748/- 1.650	0.071/.098	197/2
Cold spot 90%	2021	Dhaqar	-1.695	0.090	26

Table5. Spatial Distribution of Hot spot and Cold spot Analysis for Females (2018-2021).

Clusters Analysis	**Year's Females**	**Approximate location**	**GiZScore**	**GiPValue**	**Observed /100,000**
Hot spot 99%	2018	Diyala, Baghdad, Wasit, Babil, and Karbala	2.534	0.021	736
Hot spot 95%/ Cold spot 90%	2019	Diyala, Baghdad, Babil, and Karbala/ Basrah	2.285/ -1.647	0.023/ 0.099	575/5
Hot spot 95%/ Cold spot 90%/ Hot spot 90%	2020	Diyala, Baghdad, and Karbala/ Babil /Basrah	2.086/1.748/- 1.725	0.037/0.080 /0.084	227/91/1
Cold spot 90%/ Cold spot 90%	2021	Diyala/ Dhaqar	1.657/ -1.647	0.098/ 0.0997	173/33

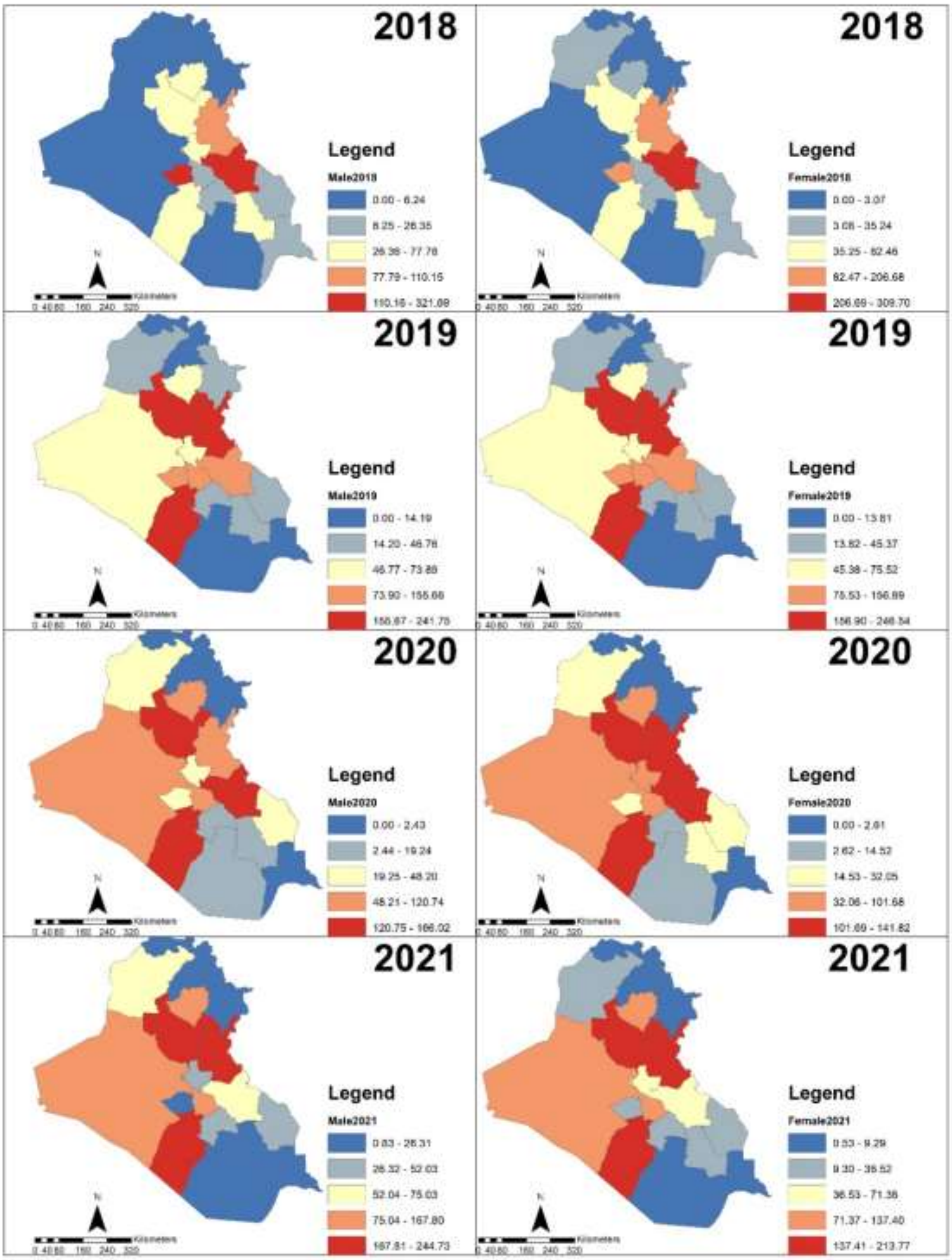

Fig. 1. Geographical distribution of hepatitis D cases per 100,000 in Iraqi provinces from 2018 to 2021 for both males (left panel) and females (right panel).

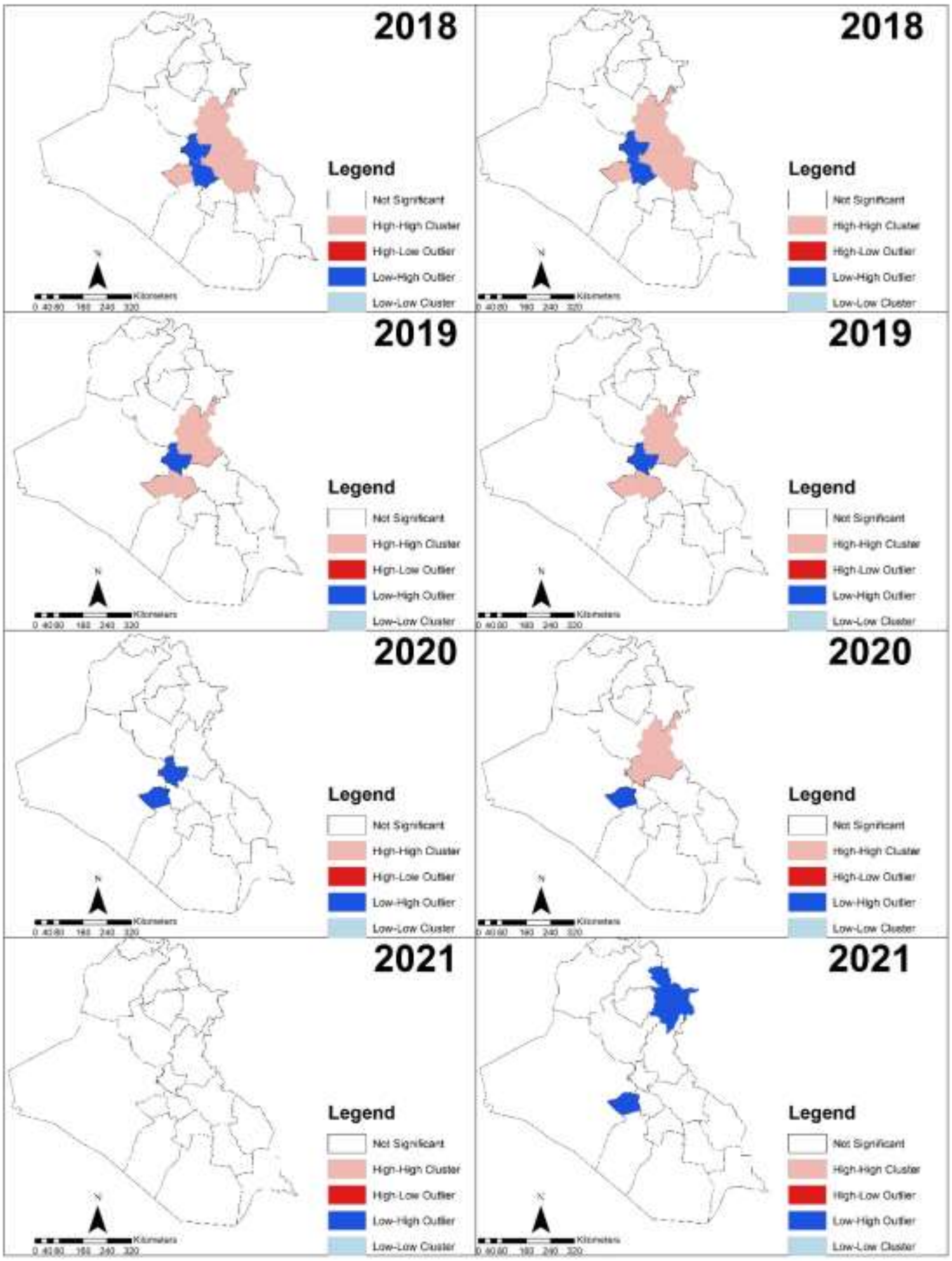

Fig.2. Clustering-outlier map of the spatial distribution of hepatitis D in males (left panel) and females (right panel) from 2018 to 2021.

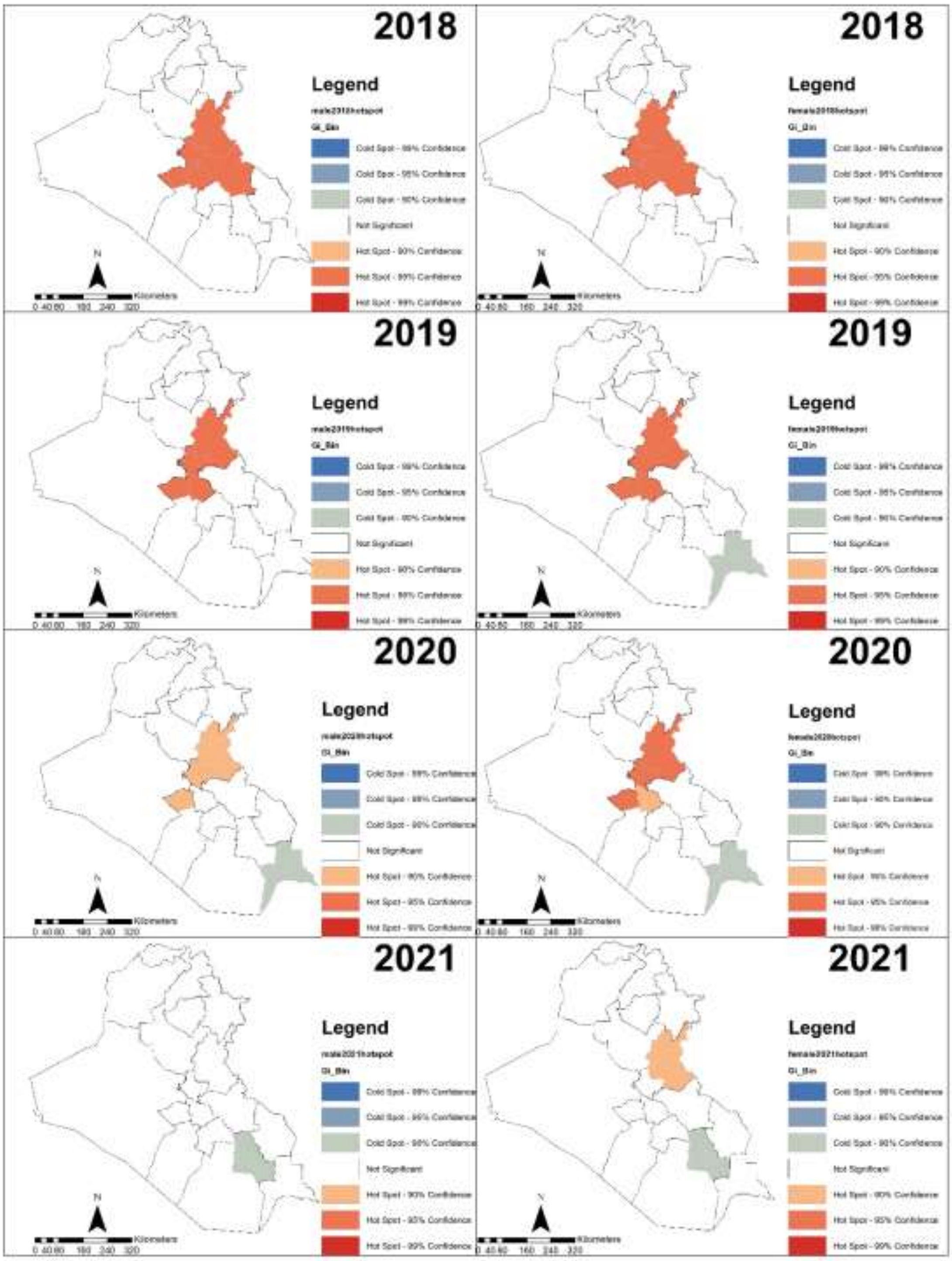

Fig.3. Hepatitis D cold hotspot analysis of the spatial distribution of males (left panel) and females (right panel) from 2018 to 2021.

V. References

1. National Development Plan (NDP). Republic of Iraq- Ministry of Planning. Baghdad: 2013.
2. World Health Organization. Hepatitis A. WHO Web Site; 2019 [updated 19 Sep 2018; cited 3 May 2019]; Available from: https://www.who.int/en/news-room/fact-sheets/detail/hepatitis-a.

3. Ginzberg D. Global HBV burden: guesstimates and facts. Hep Intl 2018, 12(4).
4. Asrani SK, Devarbhavi H, Eaton J, Kamath PS. Burden of liver diseases in the world. J Hepatol. 2019;70(1):151–71.
5. Than TT, Jo E, Todt D, Nguyen PH, Steinmann J, Steinmann E, Windisch MP. High environmental stability of hepatitis B virus and inactivation requirements for chemical biocides. J Infect Dis. 2019;219(7):1044–8.
6. Getis a, ord j. The analysis of spatial association by use of distance statistics. Geogr anal 24(3): 189–206. 1992.
7. Amiri am, nadimi n, khalifeh v, shams m. 2021. Gis-based crash hotspot identification: a comparison among mapping clusters and spatial analysis techniques. International journal of injury control and safety promotion. Https://doi.org/10.1080/17457300.2021.1925924.
8. Anselin, L. Model Validation in Spatial Econometrics: A Review and Evaluation of Alternative Approaches. Int. Reg. Sci. Rev. 1988, 11, 279–316.
9. Anselin, L. A test for spatial autocorrelation in seemingly unrelated regressions. Econ. Lett. 1988, 28, 335–341.
10. Ullah, A.; Giles, D.E.A. (Eds.) Handbook of Applied Economic Statistics; Taylor & Francis Group: New York, NY, USA, 1998; p. 624.
11. Anselin, L.; Bera, A.K.; Florax, R.; Yoon,M.J. Simple diagnostic tests for spatial dependence. Reg. Sci. Urban Econ. 1996, 26, 77–104.
12. Amaral, P.V.; Anselin, L. Finite sample properties of Moran's I test for spatial autocorrelation in tobit models. Pap. Reg. Sci. 2014, 93, 773–781.
13. Kelejian, H.; Piras, G. Tests for Spatial Correlation. In Spatial Econometrics; Kelejian, H., Piras, G., Eds.; Elsevier: Amsterdam, The Netherlands, 2017; pp. 237–270.
14. Ord, J.K.; Getis, A. Local Spatial Autocorrelation Statistics: Distributional Issues and an Application. Geogr. Anal. 1995, 27, 286–306.
15. Longley, P.; Batty, M. Spatial Analysis: Modelling in a GIS Environment; John Wiley & Sons: New York, NY, USA, 1996; p. 395.
16. Fotheringham, A.S. "The Problem of Spatial Autocorrelation" and Local Spatial Statistics. Geogr. Anal. 2009, 41, 398–403.
17. Long, J.; Robertson, C. Comparing spatial patterns. Geogr. Compass 2017, 12, 27–41.
18. ESRI. Cómo Funciona Análisis de Puntos Calientes (Gi* de Getis-Ord). Available online: https://pro.arcgis.com/es/pro-app/tool-reference/spatial-statistics/h-how-hot-spot-analysis-getis-ord-gi-spatial-stati.htm(accessed on 25 September 2018).
19. ESRI. Cómo Funciona Análisis de Cluster y de Valor Atípico (I Anselin Local de Moran). Available online: https://pro.arcgis.com/es/pro-app/tool-reference/spatial-statistics/h-how-cluster-and-outlieranalysis-anselin-local-m.htm (accessed on 25 September 2018).